Supporting Information: Unified Theory of Vapor-Wall Mass Transport in Teflon-Walled Environmental Chambers

Yuanlong Huang,[†] Ran Zhao,[‡] Sophia M. Charan,[‡] Christopher M. Kenseth,[‡] Xuan Zhang,[¶] and John H. Seinfeld[*,‡,§]

[†]*Division of Geological and Planetary Sciences, California Institute of Technology, Pasadena, CA, USA, 91125*

[‡]*Division of Chemistry and Chemical Engineering, California Institute of Technology, Pasadena, CA, USA, 91125*

[¶]*National Center for Atmospheric Research, Boulder, CO, USA, 80301*

[§]*Division of Engineering and Applied Science, California Institute of Technology, Pasadena, CA, USA, 91125*

E-mail: seinfeld@caltech.edu

Phone: +1 626 395 4635. Fax: +1 626 568 8743

This Supporting Information has 27 pages, including 5 figures and 1 long table.

Contents:

I. Gas-Phase Boundary Layer Transport

The governing equation for gas-phase boundary layer mass transport of a tracer molecule of concentration C_g^δ across a layer of thickness δ on the wall of a chamber is :

$$\frac{\partial C_g^\delta}{\partial t} = \frac{\partial}{\partial x}\left[(\mathcal{D}_g + k_e x^2)\frac{\partial C_g^\delta}{\partial x}\right] = (\mathcal{D}_g + k_e x^2)\frac{\partial^2 C_g^\delta}{\partial x^2} + 2xk_e\frac{\partial C_g^\delta}{\partial x} \tag{S1}$$

where $\mathcal{D}_g$ is the vapor molecular diffusivity in the gas phase, and k_e is the eddy diffusivity coefficient characteristic of mixing in the bulk of the chamber.[1,2]

The boundary condition at the outer extent of the boundary layer, $x = \delta$, is:

$$C_g^\delta(\delta, t) = C_g^b(t) \tag{S2}$$

where $C_g^b(t)$ is the concentration in the bulk of the chamber.

The rate of change of $C_g^b(t)$ owing to removal from the bulk by transport to and uptake by the chamber wall is:

$$V\frac{dC_g^b(t)}{dt} = -A\left[(\mathcal{D}_g + k_e x^2)\frac{\partial C_g^\delta}{\partial x}\right]\Bigg|_{x=\delta} \tag{S3}$$

where V and A are the volume and surface area of the chamber, respectively.

The boundary condition on C_g^δ at the wall surface, $x = 0$, owing to equality of fluxes, is:

$$\mathcal{D}_g\left(\frac{\partial C_g^\delta}{\partial x}\right)\Bigg|_{x=0} = \frac{\alpha_w\omega}{4}\left(C_g^\delta\big|_{x=0} - \frac{C_s}{K_w}\right) \tag{S4}$$

where α_w is the accommodation coefficient at the wall, ω is the mean molecular velocity of the species, and $K_w = \dfrac{C_w}{\gamma^\infty c^*}$. γ^∞ is the activity coefficient of vapor molecules dissolved in the wall, c^* is the species mass saturation concentration, C_w is the effective organic mass concentration of the wall, by analogy to the effective aerosol mass concentration used in describing vapor-particle uptake,[3] and C_s is the species concentration uniformly dissolved in

the wall surface layer.

Correspondingly, the rate of change of $C_s(t)$ is:

$$V\frac{dC_s(t)}{dt} = A\left[(\mathcal{D}_g + k_e x^2)\left(\frac{\partial C_g^\delta}{\partial x}\right)\right]\Bigg|_{x=0} \tag{S5}$$

The concentration profile of vapors in the boundary layer will eventually relax to a quasi-steady state, under which the governing equation for the gas-phase concentration reduces to:

$$0 = \frac{\partial}{\partial x}\left[(\mathcal{D}_g + k_e x^2)\frac{\partial C_g^\delta}{\partial x}\right] \tag{S6}$$

The boundary conditions on Eq. (S6) are $C_g^\delta(\delta, t) = C_g^b(t)$ and $C_g^\delta(0, t) = C_{g,0}^\delta(t)$, where $C_{g,0}^\delta(t)$ is the gas-phase concentration immediately above the wall surface. Note that the time t refers to that in the period after which quasi-steady state conditions have been reached. The solution to Eq. (S6) subject to its boundary conditions is:

$$C_g^\delta(x,t) = \left(C_g^b(t) - C_{g,0}^\delta(t)\right)\arctan\left(x\sqrt{\frac{k_e}{\mathcal{D}_g}}\right)/\arctan\left(\delta\sqrt{\frac{k_e}{\mathcal{D}_g}}\right) + C_{g,0}^\delta(t) \tag{S7}$$

The rates of change of $C_g^b(t)$ and $C_s(t)$ over the entire chamber are:

$$\begin{aligned} V\frac{dC_g^b(t)}{dt} &= -A\left[(\mathcal{D}_g + k_e x^2)\frac{\partial C_g^\delta}{\partial x}\right]\Bigg|_{x=\delta} \\ &= -\left(C_g^b(t) - C_{g,0}^\delta(t)\right)\sqrt{k_e\mathcal{D}_g}/\arctan\left(\delta\sqrt{\frac{k_e}{\mathcal{D}_g}}\right) = -\frac{\alpha_w\omega}{4}\left(C_{g,0}^\delta(t) - \frac{C_s(t)}{K_w}\right) \\ &= -A\,\mathcal{D}_g\left(\frac{\partial C_g^\delta}{\partial x}\right)\Bigg|_{x=0} = -V\frac{dC_s(t)}{dt} \end{aligned} \tag{S8}$$

Since $C_{g,0}^\delta(t)$ is unknown, we can rewrite Eq. (S8) as:

$$\frac{dC_g^b(t)}{dt} = -\left(\frac{A}{V}\right)\left(\frac{1}{v_e} + \frac{1}{v_c}\right)^{-1}\left(C_g^b(t) - \frac{C_s(t)}{K_w}\right) = -\frac{dC_s(t)}{dt} \tag{S9}$$

where $v_e = \sqrt{k_e \mathcal{D}_g}/\arctan\left(\delta\sqrt{\frac{k_e}{\mathcal{D}_g}}\right)$ and $v_c = \frac{\alpha_w \omega}{4}$. Under typical chamber conditions, $\frac{\delta^2 k_e}{\mathcal{D}_g} \gg 1$, $v_e = \frac{2}{\pi}\sqrt{k_e \mathcal{D}_g}$. The initial condition is: at $t = 0$, $C_g^b = C_{g0}^b$ and $C_s = 0$. From Eq. (S9), we can solve for the time evolution of C_g^b and C_s.

If we define $\Delta C(t) = C_g^b(t) - \frac{C_s(t)}{K_w}$ as the deviation from equilibrium, we can derive the rate of change of $\Delta C(t)$ from Eq. (S9):

$$\frac{d\Delta C(t)}{dt} = \frac{d\left[C_g^b(t) - \frac{C_s(t)}{K_w}\right]}{dt} = -\left(\frac{A}{V}\right)\left(1 + \frac{1}{K_w}\right)\left(\frac{1}{v_e} + \frac{1}{v_c}\right)^{-1}\Delta C(t) \tag{S10}$$

So the vapor-wall equilibration time scale (τ_{vwe})is:

$$\tau_{vwe} = \left(\frac{A}{V}\right)^{-1}\left(1 + \frac{1}{K_w}\right)^{-1}\left(\frac{1}{v_e} + \frac{1}{v_c}\right) \tag{S11}$$

The two key parameters in the vapor-wall interaction are the accommodation coefficient on the wall α_w and the vapor-wall equilibrium constant K_w. Of interest is the extent to which α_w and K_w impact the time for the gas-phase concentration to reach quasi-steady state within the boundary layer. For example, for the Caltech chamber, the eddy diffusion coefficient $k_e = 0.075$ (s^{-1}),[4] and $\frac{A}{V} = 2.08$ (m^{-1}); we assume $\mathcal{D}_g = 5 \times 10^{-6}$ (m^2 s^{-1}), and $\omega = 200$ (m s^{-1}). To satisfy the condition $\frac{\delta^2 k_e}{\mathcal{D}_g} \gg 1$, the boundary layer thickness δ is on the order of 10^{-1} m.[1] We will consider as well δ values of 10^{-2} and 10^0 m. α_w and K_w are varied to estimate the time scale for the gas-phase concentration to reach 95% of its quasi-steady state profile with the boundary layer thickness $\delta = 10^{-1}$, 10^{-2}, and 10^0 m, respectively.

The time scales are shown in Fig. S1, indicating that for a wide range of boundary layer thickness δ, the gas-phase boundary layer reaches quasi-steady state within ~ 10 s. Based on this conclusion, it is reasonable to use the quasi-steady-state flux directly in calculations.

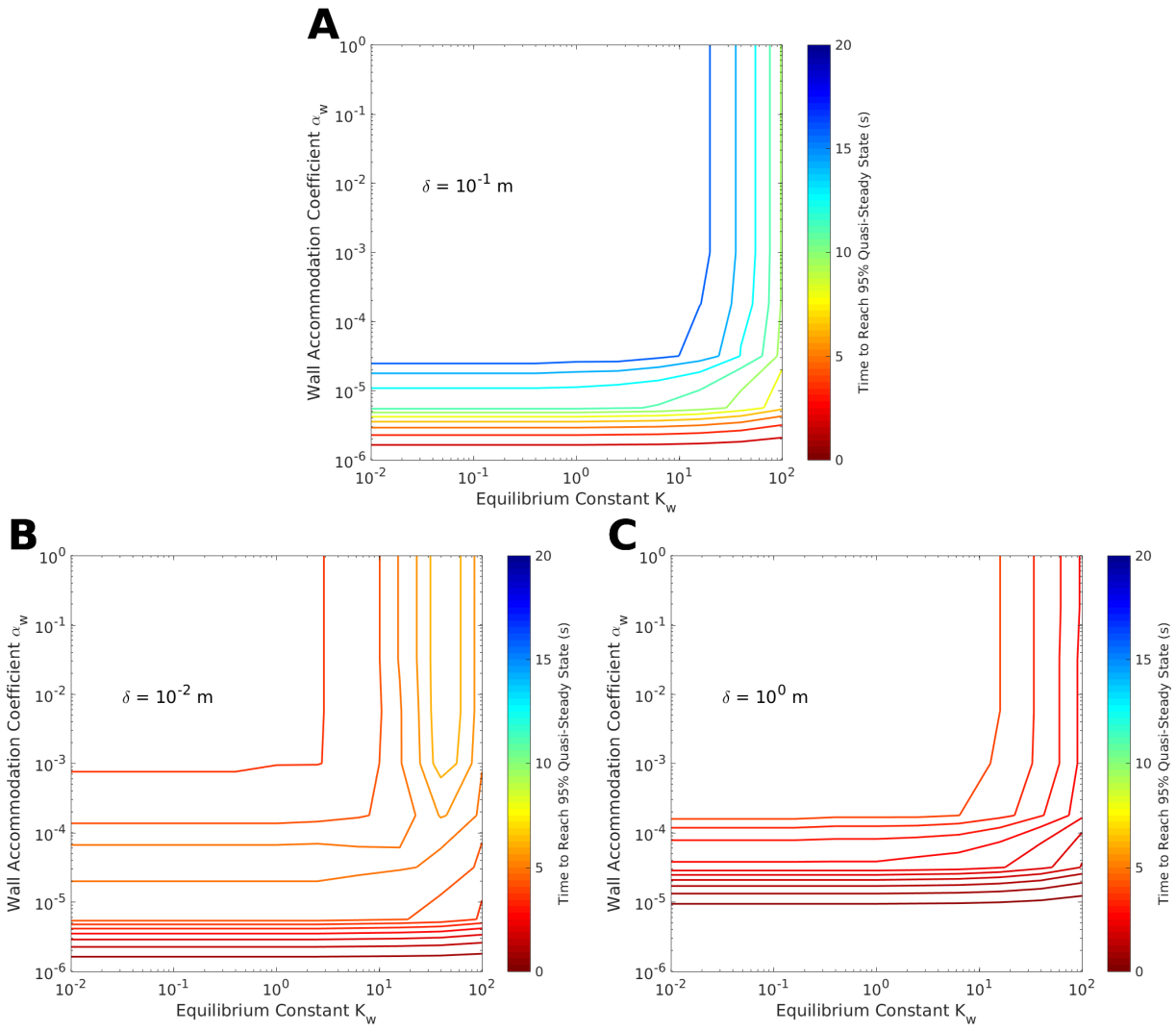

Figure S1: Time scale for gas-phase concentration to reach 95% of the quasi-steady state in a boundary layer of thickness of (A) $\delta = 0.1$ m, (B) $\delta = 0.01$ m, and (C) $\delta = 1$ m.

II. Activity and Accommodation Coefficients

This section addresses the information used to calculate γ^{∞} and α_w based on data from the literature.[5–8]

The activity coefficient γ^{∞} in Teflon film can be calculated by the following equation:

$$\gamma^{\infty} = \frac{MW_{voc}}{MW_w} \cdot \frac{C_w}{c^* \cdot C_s/C_g} \tag{S12}$$

where MW_{voc} and MW_w are the molecular weight of the compound (varies, listed in the following table) and the wall (assumed 200 g mol^{-1}),[5] C_w is the equivalent wall mass concentration (e.g., 32.2 mg m^{-3} for the chambers used by Krechmer et al.[8] and Ziemann et al.[6,7]), c^* is the saturation concentration (μg m^{-3}, estimated by EVAPORATION[9]), and C_s/C_g is the ratio of vapor concentration dissolved in the wall surface layer to that in the gas phase at equilibrium (data from the literature[5–8]). See the caption of Fig. S2 for details.

The characteristic equilibration timescale τ_{vwe} for gas-wall partitioning is:

$$\tau_{vwe} = \frac{1}{k_{g\rightarrow w} + k_{g\leftarrow w}} = \frac{1}{k_{g\rightarrow w}} \frac{1}{1 + 1/K_{eq}} \tag{S13}$$

where $k_{g\rightarrow w} = \left(\frac{A}{V}\right)\left(\frac{4}{\alpha_w \omega} + \frac{\pi}{2}\frac{1}{\sqrt{k_e \mathcal{D}_g}}\right)^{-1}$, $K_{eq} = \frac{k_{g\rightarrow w}}{k_{g\leftarrow w}} = \left(\frac{C_s}{C_g}\right)_{eq}$, and $\omega = \sqrt{\frac{8RT}{\pi MW_{voc}}}$, R is the gas constant, and T is temperature. Both the gas-to-wall transfer constant $k_{g\rightarrow w}$ and the equilibrium constant K_{eq} determine the characteristic timescale τ_{vwe}. $k_{g\rightarrow w}$ is determined by both the surface accommodation coefficient α_w and the eddy diffusivity k_e in the chamber. For either monofunctional or multifunctional compounds, Krechmer et al.[8] recommended constant timescales (1800 s and 600 s) in the same chamber simulation, even though the equilibrium constants are different. Such an assumption (τ_{vwe} is fixed, but K_{eq} varies) requires that the accommodation coefficient α_w is compound-dependent.

We can calculate the surface accommodation coefficient α_w with the following equation

derived from EQ. (S13):

$$\alpha_w = \frac{4}{\omega}\left[\tau_{vwe}\left(\frac{A}{V}\right)\left(1+\frac{1}{C_s/C_g}\right)-\frac{\pi}{2}\frac{1}{\sqrt{k_e\mathcal{D}_g}}\right]^{-1} \tag{S14}$$

Estimates of the characteristic timescale τ_{vwe} and the ratio C_s/C_g at equilibrium can be obtained from measurements in the literature.[5–8] Krechmer et al.[8] suggested the eddy diffusivity k_e could be calculated by:

$$k_e = 0.004 + 5.6 \times 10^{-3} V^{0.74} \tag{S15}$$

With a chamber volume of $V = 8$ m^3, $k_e = 0.03$ s^{-1}. The gas-phase diffusivity $\mathcal{D}_g$ is set as a constant 5×10^{-6} m^2 s^{-1} for all compounds. The calculated values of α_w are listed in Table. S1 and shown in Fig. S3. An empirical equation fitted to the data clearly indicates a negative dependence of α_w on the vapor saturation concentration, which is consistent with the expectation that less volatile compounds are more "sticky". Note that when $k_e = 0.03$ s^{-1}, negative values of α_w result from the NO_3^--CIMS data,[8] suggesting that under their chamber conditions, the limiting step is gas-phase boundary layer diffusion (Fig. S3, left upper grean area), which was verified by turning on the fan inside the chamber (so that k_e increases) leading to a much faster decay rate. For the Caltech chamber, $k_e = 0.075$ s^{-1}, calculated based on the particle-wall deposition rate,[4] yields a critical $\alpha_w = 7.80 \times 10^{-6}$ ($\omega = 200$ m s^{-1}), corresponding to $c^* = 4 \times 10^3$ μg m^{-3} from the fitting expression (Fig. S3). The range of saturation concentration c^* of the compounds studied by Zhang et al.[10] is $10^{-1} - 10^6$ μg m^{-3}. We apply this fitting expression (Fig. S3) to predict α_w.

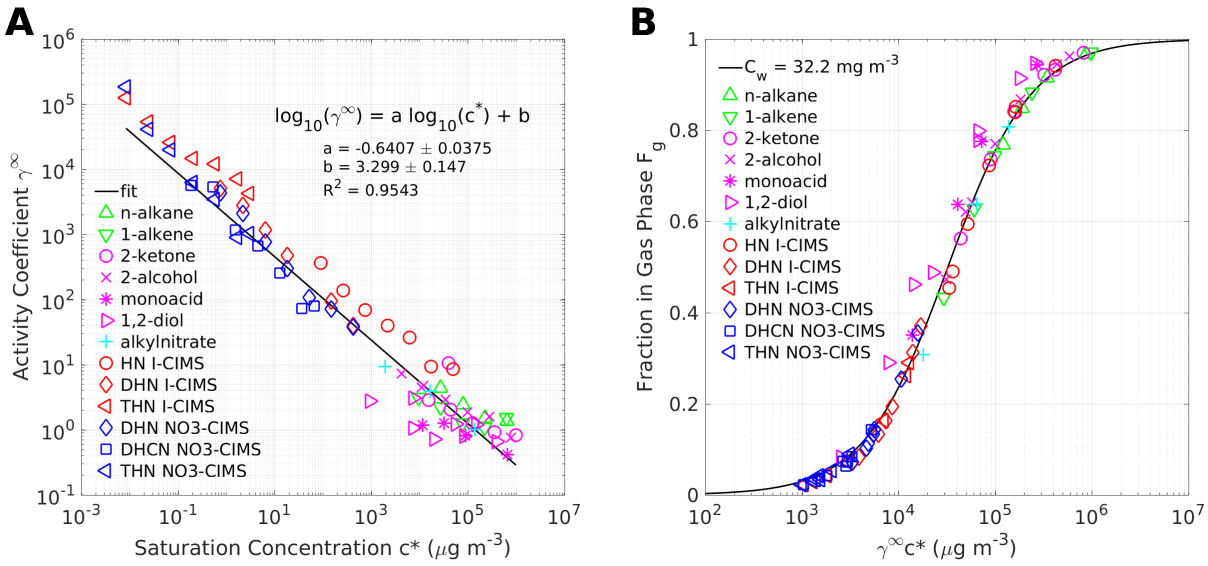

Figure S2: Panel (A) Activity coefficients γ^{∞} in FEP film calculated from the literature[5–8] as a function of vapor saturation concentration (c^*) estimated by EVAPORATION.[9,11] Raw data used to calculate γ^{∞} are provided in Table S1. n-alkanes and 1-alkenes (green) are from Matsunaga and Ziemann.[5] 2-ketones, 2-alcohols, monoacids, and 1,2-diols (magenta) are from Yeh and Ziemann.[7] Alkylnitrates (cyan) are from Yeh and Ziemann.[6] I^--CIMS (red) and NO_3^--CIMS (blue) are from Krechmer et al..[8] SIMPOL.1[12] predicts vapor pressure by summation of group contributions, and EVAPORATION considers group position effect for multifunctional isomers. The difference in vapor pressure estimated by these two methods is within a factor of $2 \sim 3$. For multifunctional isomers, all HNs[8] (hydroxynitrates) are 1-OH-5-alkylnitrates, DHNs (dihydroxynitrates) are 1,5-OH-2-alkylnitrates, THNs (trihydroxynitrates) are 1,2,5-OH-6-alkylnitrates, and DHCNs (dihydroxycarbonylnitrates) are 1,2-OH-5-carbonyl-6-alkylnitrates. Measurements by I^--CIMS[8] are thought to be biased by "memory" effects arising from sampling tube and instrument inlet; thus, they are excluded in the fitting. Panel (B) Fraction F_g at vapor-wall equilibrium remaining in the gas phase[8] as a function of $\gamma^{\infty}c^*$. $F_g = \dfrac{1}{1 + C_w/(\gamma^{\infty}c^*)}$, where $C_w = 32.2$ mg m^{-3} corresponding to $L_e = 5$ nm and surface-to-volume ratio $\dfrac{A}{V} = 3$ m^{-1}.

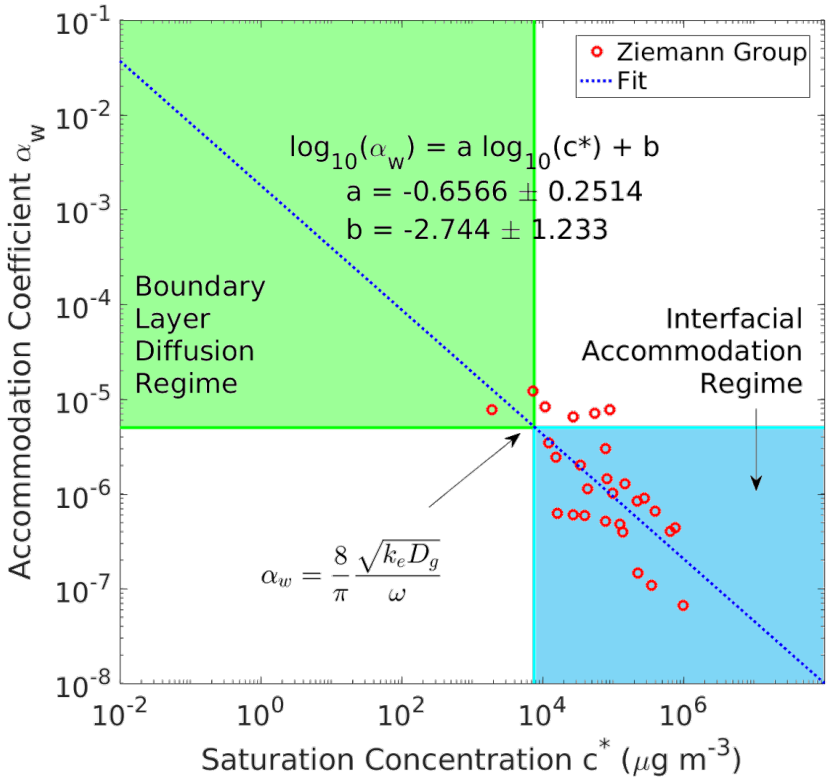

Figure S3: Accommodation coefficient of vapor molecules on the Teflon wall α_w versus saturation concentration c^*. Data are from the Ziemann group.[5–7] An empirical relationship is fitted to the data points. The critical α_w point[13] (5.12×10^{-6}, corresponding to $k_e = 0.03$ s^{-1}, marked by an arrow) is that at which the rate of mass transport to the wall shifts from the gas-phase boundary layer diffusion regime (green area) to the interfacial accommodation regime (blue area). The fitted line indicates that the compounds studied by Krechmer et al.[8] (c^* in the range of $10^{-2} - 10^4$ μg m^{-3}) lie in the gas-phase boundary layer diffusion regime.

Table S1: Literature data used to calculated activity coefficient γ^{∞} and accommodation coefficient α_w

	T	$\mathcal{D}_g$	L_e	ρ_{FEP}	A/V	V	MW_{FEP}	C_w^{eq}
	(K)	(m^2 s^{-1})	(nm)	(kg m^{-3})	(m^{-1})	(m^3)	(g mol^{-1})	(μg m^{-3})
	298	5×10^{-6}	5	2150	3	8	200	3.22E+04

				min	g mol^{-1}	atm		
2-ketone[7]		F_g	C_w/C_g	τ_{vwe}	MW_{voc}	EVAPORATION	α_w	γ^{∞}
	2-decanone	0.970	0.031	50	156	1.55E-04	6.72E-08	8.24E-01
	2-undecanone	0.921	0.085	85	170	5.06E-05	1.09E-07	9.14E-01
	2-dodecanone	0.841	0.188	43	184	1.65E-05	4.83E-07	1.26E+00
	cyclododecanone	0.933	0.072	15	184	5.23E-06	5.96E-07	1.05E+01
	2-tridecanone	0.736	0.359	35	198	5.41E-06	1.13E-06	2.03E+00
	2-tetraecanone	0.563	0.776	33	212	1.77E-06	2.43E-06	2.87E+00

				min	g mol^{-1}	atm		
2-alcohol[7]		F_g	C_w/C_g	τ_{vwe}	MW_{voc}	EVAPORATION	α_w	γ^{∞}
	2-nonanol	0.962	0.040	10	144	1.31E-04	4.41E-07	7.65E-01
	2-decanol	0.945	0.058	8	158	4.27E-05	9.04E-07	1.59E+00
	2-undecanol	0.868	0.152	18	172	1.40E-05	1.02E-06	1.86E+00
	2-dodecanol	0.770	0.300	19	186	4.56E-06	2.01E-06	2.89E+00
	cyclododecanol	0.621	0.610	14	186	1.44E-06	8.36E-06	4.48E+00
	2-tridecanol	0.642	0.558	21	200	1.49E-06	3.46E-06	4.74E+00
	2-tetradecanol	0.473	1.114	-	214	4.88E-07	-	7.25E+00

				min	g mol^{-1}	atm		
monoacid[7]		F_g	C_w/C_g	τ_{vwe}	MW_{voc}	EVAPORATION	α_w	γ^∞
	pentanoic acid	0.943	0.060	14	102	1.57E-04	4.01E-07	4.15E-01
	heptanoic acid	0.775	0.290	8	130	1.68E-05	7.73E-06	8.09E-01
	octanoic acid	0.637	0.570	-	144	5.49E-06	-	1.26E+00
	nonanoic acid	0.351	1.849	-	158	1.80E-06	-	1.19E+00

				min	g mol^{-1}	atm		
1,2-diol[7]		F_g	C_w/C_g	τ_{vwe}	MW_{voc}	EVAPORATION	α_w	γ^∞
	1,2-butanediol	0.947	0.056	8	90	1.06E-04	6.53E-07	6.62E-01
	1,2-pentanediol	0.914	0.094	8	104	3.48E-05	1.28E-06	1.20E+00
	1,4-pentanediol	0.799	0.252	17	104	1.95E-05	1.45E-06	8.05E-01
	1,5-pentanediol	0.462	1.165	-	104	4.68E-06	-	7.23E-01
	1,2-hexanediol	0.778	0.285	8	118	1.14E-05	7.10E-06	1.21E+00
	1,6-hexanediol	0.290	2.448	-	118	1.53E-06	-	1.05E+00
	1,2-octanediol	0.488	1.049	16	146	1.22E-06	1.22E-05	3.09E+00
	1,8-octanediol	0.010	95.618	-	146	1.64E-07	-	2.52E-01
	1,2-decanediol	0.083	11.048	-	174	1.30E-07	-	2.74E+00
	1,10-decanediol	0.010	98.010	-	174	1.75E-08	-	2.30E+00

				min	g mol^{-1}	atm		

alkane[5]		F_g	C_w/C_g	τ_{vwe}	MW_{voc}	EVAPORATION	α_w	γ^∞
	N-tridecane	0.967	0.034	-	184	8.47E-05	-	1.36E+00
	N-tetradecane	0.915	0.093	74	198	2.77E-05	1.48E-07	1.52E+00
	N-pentadecane	0.848	0.180	41	212	9.06E-06	5.18E-07	2.42E+00
	N-hexadecane	0.767	0.303	56	226	2.96E-06	6.06E-07	4.39E+00
				min	g mol^{-1}	atm		
alkene[5]		F_g	C_w/C_g	τ_{vwe}	MW_{voc}	EVAPORATION	α_w	γ^∞
	1-tridecene	0.971	0.030	-	182	8.47E-05	-	1.55E+00
	1-tetradecene	0.884	0.132	20	196	2.77E-05	8.42E-07	1.08E+00
	1-pentadecene	0.744	0.345	17	210	9.06E-06	2.99E-06	1.26E+00
	1-hexadecene	0.627	0.595	16	224	2.96E-06	6.52E-06	2.24E+00
	1-heptadecene	0.433	1.311	-	238	9.68E-07	-	3.11E+00
				min	g mol^{-1}	atm		
alkylnitrate[6]		F_g	C_w/C_g	τ_{vwe}	MW_{voc}	EVAPORATION	α_w	γ^∞
	2-decyl nitrate	0.807	0.239	65	203	1.64E-05	3.99E-07	1.00E+00
	2-dodecyl nitrate	0.638	0.568	85	227	1.76E-06	6.24E-07	3.95E+00
	2-tetradecyl nitrate	0.307	2.252	28	251	1.88E-07	7.71E-06	9.32E+00
				min	g mol^{-1}	atm		
HN I^--CIMS[8]		F_g	C_w/C_g	τ_{vwe}	MW_{voc}	EVAPORATION	α_w	γ^∞
	$C_6H_{13}NO_4$	0.941	0.063	-	163	7.36E-06	-	8.56E+00

	$C_7H_{15}NO_4$	0.851	0.175	-	177	2.41E-06	-	9.39E+00
	$C_8H_{17}NO_4$	0.839	0.192	-	191	7.87E-07	-	2.62E+01
	$C_9H_{19}NO_4$	0.723	0.383	-	205	2.57E-07	-	4.00E+01
	$C_{10}H_{21}NO_4$	0.594	0.684	-	219	8.41E-08	-	6.87E+01
	$C_{11}H_{23}NO_4$	0.490	1.041	-	233	2.75E-08	-	1.38E+02
	$C_{12}H_{25}NO_4$	0.454	1.203	-	247	8.99E-09	-	3.64E+02

				min	g mol^{-1}	atm		
DHN I$^-$-CIMS[8]		F_g	C_w/C_g	τ_{vwe}	MW_{voc}	EVAPORATION	α_w	γ^∞
	$C_6H_{13}NO_5$	0.371	1.695	-	179	5.77E-08	-	4.03E+01
	$C_7H_{15}NO_5$	0.312	2.205	-	193	1.89E-08	-	9.48E+01
	$C_9H_{19}NO_5$	0.194	4.155	-	221	2.02E-09	-	4.71E+02
	$C_{10}H_{21}NO_5$	0.163	5.135	-	235	6.59E-10	-	1.17E+03
	$C_{11}H_{23}NO_5$	0.133	6.519	-	249	2.16E-10	-	2.80E+03
	$C_{12}H_{25}NO_5$	0.083	11.048	-	263	7.05E-11	-	5.06E+03

				min	g mol^{-1}	atm		
THN I$^-$-CIMS[8]		F_g	C_w/C_g	τ_{vwe}	MW_{voc}	EVAPORATION	α_w	γ^∞
	$C_6H_{13}NO_6$	0.290	2.448	-	195	3.79E-10	-	4.26E+03
	$C_7H_{15}NO_6$	0.262	2.817	-	209	1.96E-10	-	7.15E+03
	$C_8H_{17}NO_6$	0.163	5.135	-	223	6.42E-11	-	1.20E+04
	$C_9H_{19}NO_6$	0.072	12.831	-	237	2.10E-11	-	1.46E+04
	$C_{10}H_{21}NO_6$	0.043	22.364	-	251	6.86E-12	-	2.57E+04

	$C_{11}H_{23}NO_6$	0.030	32.898	-	265	2.24E-12	-	5.33E+04
	$C_{12}H_{25}NO_6$	0.023	42.860	-	279	7.34E-13	-	1.25E+05

				min	g mol^{-1}	atm		
DHN NO_3^--CIMS[8]		F_g	C_w/C_g	τ_{vwe}	MW_{voc}	EVAPORATION	α_w	γ^∞
	$C_6H_{13}NO_5$	0.355	1.817	9	179	5.77E-08	-	3.76E+01
	$C_7H_{15}NO_5$	0.254	2.937	11.8	193	1.89E-08	-	7.13E+01
	$C_8H_{17}NO_5$	0.143	5.993	11.2	207	6.17E-09	-	1.07E+02
	$C_9H_{19}NO_5$	0.133	6.519	12.6	221	2.02E-09	-	2.99E+02
	$C_{10}H_{21}NO_5$	0.114	7.772	10.2	235	6.59E-10	-	7.68E+02
	$C_{11}H_{23}NO_5$	0.103	8.709	11.8	249	2.16E-10	-	2.10E+03
	$C_{12}H_{25}NO_5$	0.072	12.831	9.8	263	7.05E-11	-	4.36E+03

				min	g mol^{-1}	atm		
DHCN NO_3^--CIMS[8]		F_g	C_w/C_g	τ_{vwe}	MW_{voc}	EVAPORATION	α_w	γ^∞
	$C_6H_{11}NO_6$	0.143	5.993	8.2	193	8.35E-09	-	7.89E+01
	$C_7H_{13}NO_6$	0.074	12.587	10	207	4.32E-09	-	7.25E+01
	$C_8H_{15}NO_6$	0.084	10.862	8.6	221	1.41E-09	-	2.57E+02
	$C_9H_{17}NO_6$	0.072	12.831	9.4	235	4.62E-10	-	6.65E+02
	$C_{10}H_{19}NO_6$	0.043	22.364	8	249	1.51E-10	-	1.17E+03
	$C_{11}H_{21}NO_6$	0.063	14.898	9	263	4.94E-11	-	5.36E+03
	$C_{12}H_{23}NO_6$	0.023	42.860	7.4	277	1.62E-11	-	5.68E+03

				min	g mol^{-1}	atm		
THN NO_3^--CIMS[8]		F_g	C_w/C_g	τ_{vwe}	MW_{voc}	EVAPORATION	α_w	γ^∞
	$C_6H_{13}NO_6$	0.090	10.148	10.2	195	3.79E-10	-	1.02E+03
	$C_7H_{15}NO_6$	0.043	22.364	11.2	209	1.96E-10	-	8.99E+02
	$C_8H_{17}NO_6$	0.054	17.692	9.4	223	6.42E-11	-	3.48E+03
	$C_9H_{19}NO_6$	0.032	30.153	11.4	237	2.10E-11	-	6.24E+03
	$C_{10}H_{21}NO_6$	0.034	28.851	9.8	251	6.86E-12	-	1.99E+04
	$C_{11}H_{23}NO_6$	0.023	42.860	11.6	265	2.24E-12	-	4.09E+04
	$C_{12}H_{25}NO_6$	0.034	28.851	10.4	279	7.34E-13	-	1.86E+05

III. Analytical Solution for the Kinetics of the System $\mathbf{G} \xrightarrow{\mathbf{k_0}} \mathbf{X} \underset{\mathbf{k_{-1}}}{\overset{\mathbf{k_1}}{\rightleftharpoons}} \mathbf{Y}$

The system dynamics are described by the set of linear ODEs:

$$\frac{d}{dt}\mathbf{W} = \mathbb{A} \cdot \mathbf{W} \tag{S16}$$

where $\mathbf{W} = \begin{pmatrix} G \\ X \\ Y \end{pmatrix}$, $\mathbb{A} = \begin{pmatrix} -k_0 & 0 & 0 \\ k_0 & -k_1 & k_{-1} \\ 0 & k_1 & -k_{-1} \end{pmatrix}$. The initial condition is $\mathbf{W}_0 = \begin{pmatrix} G_0 \\ 0 \\ 0 \end{pmatrix}$. The eigenvalues of $\mathbb{A}$ are $\lambda_1 = -k_0$, $\lambda_2 = 0$, and $\lambda_3 = -(k_1 + k_{-1})$.

When $k_0 \neq k_1 + k_{-1}$, the analytical solution for the concentrations of the three species is:

$$\frac{1}{G_0}\mathbf{W} = \begin{pmatrix} 1 \\ \dfrac{-k_0 + k_{-1}}{k_0 - k_1 - k_{-1}} \\ \dfrac{k_1}{k_0 - k_1 - k_{-1}} \end{pmatrix} \mathrm{e}^{-k_0 t} + \begin{pmatrix} 0 \\ \dfrac{k_{-1}}{k_1 + k_{-1}} \\ \dfrac{k_1}{k_1 + k_{-1}} \end{pmatrix} + \begin{pmatrix} 0 \\ \dfrac{k_0 k_1/(k_1 + k_{-1})}{k_0 - k_1 - k_{-1}} \\ -\dfrac{k_0 k_1/(k_1 k_{-1})}{k_0 - k_1 - k_{-1}} \end{pmatrix} \mathrm{e}^{-(k_1 + k_{-1})t} \tag{S17}$$

When $k_0 = k_1 + k_{-1}$, the solution is:

$$\frac{1}{G_0}\mathbf{W} = \begin{pmatrix} 1 \\ -\dfrac{k_{-1}}{k_1 + k_{-1}} \\ -\dfrac{k_1}{k_1 + k_{-1}} \end{pmatrix} \mathrm{e}^{-k_0 t} + \begin{pmatrix} 0 \\ \dfrac{k_{-1}}{k_1 + k_{-1}} \\ \dfrac{k_1}{k_1 + k_{-1}} \end{pmatrix} + \begin{pmatrix} 0 \\ \dfrac{k_0 k_1}{k_1 + k_{-1}} \\ -\dfrac{k_0 k_1}{k_1 + k_{-1}} \end{pmatrix} t\mathrm{e}^{-(k_1 + k_{-1})t} \tag{S18}$$

After the oxidation period of duration t_0, during which G is oxidized to X, $X(t_0) + Y(t_0) = X_e + Y_e = 1 - \mathrm{e}^{-k_0 t_0}$, where X_e and Y_e are equilibrium concentrations of X and Y and have

a relationship of $\frac{Y_e}{X_e} = K = \frac{k_1}{k_{-1}}$. Thus the derivation from equilibrium $\epsilon(t_0, K)$ is

$$\epsilon(t_0, K) = \frac{X(t_0) - X_e}{Y_e} = \frac{X(t_0) - (1 - \mathrm{e}^{-k_0 t_0})\frac{1}{1+K}}{(1 - \mathrm{e}^{-k_0 t_0})\frac{K}{1+K}} \tag{S19}$$

IV. Fresh versus Aged Teflon Chambers

Ratios of the inferred molecular diffusivities in fresh vs. aged Teflon as a function of c^* are shown in Fig. S4, based on the measurements of Zhang et al.[10] It is found that the inferred diffusivity in fresh Teflon chambers is ~ 1 order of magnitude lower than that in an aged chamber. No apparent trend for high-NO_x and low-NO_x conditions is evident. Over 330 experiments were carried out in the "aged" Caltech chambers from 2012 to 2014, whereas the "fresh" data were obtained immediately after installation of new chambers. A change in polymer diffusivity over time has been reported,[14] attributed to unrecoverable inter-chain bonds, such that subsequent diffusion events are characterized by internal stress relaxation.[15]

Differences in measured vapor-wall deposition rates between fresh and aged Teflon chambers are consistent with the observations by Loza et al.[16] that the first-order vapor-wall loss rate is essentially negligible in new chambers but increases as more and more experiments are performed. However, this observation is not in conflict with that by Matsunaga and Ziemann[5] of a lack of chamber age dependence for surface layer absorption,[15] since the surface layer, i.e. the sharp and swollen boundary interface, is the same in either fresh or aged Teflon chambers.

The effect of temperature on vapor-wall deposition was studied at 45°C and 20°C for three relatively volatile species (isoprene, MACR, and MVK, Fig. S4). The data indicate that at higher temperature, these three species exhibit a slower wall deposition rate. The reason is unclear; it could be a result of decreased surface accommodation at higher temperature, as parameterized by α_w.

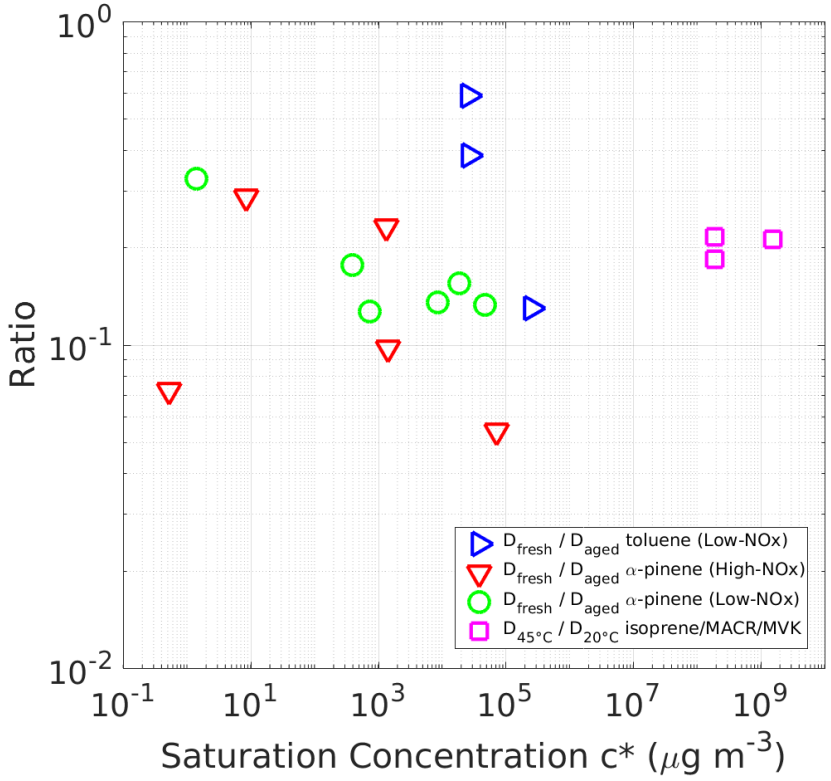

Figure S4: Ratio of inferred diffusivity in fresh to aged Teflon film as well as that at 45°C to 20°C as a function of saturation concentration c^*. Since the wall accommodation coefficient, α_w, at 45°C is assumed the same as that at 20°C, the smaller inferred diffusivity at 45°C could also be caused by lower α_w at higher temperature.

V. Humidity Effect on Teflon Inner Layer Diffusivity

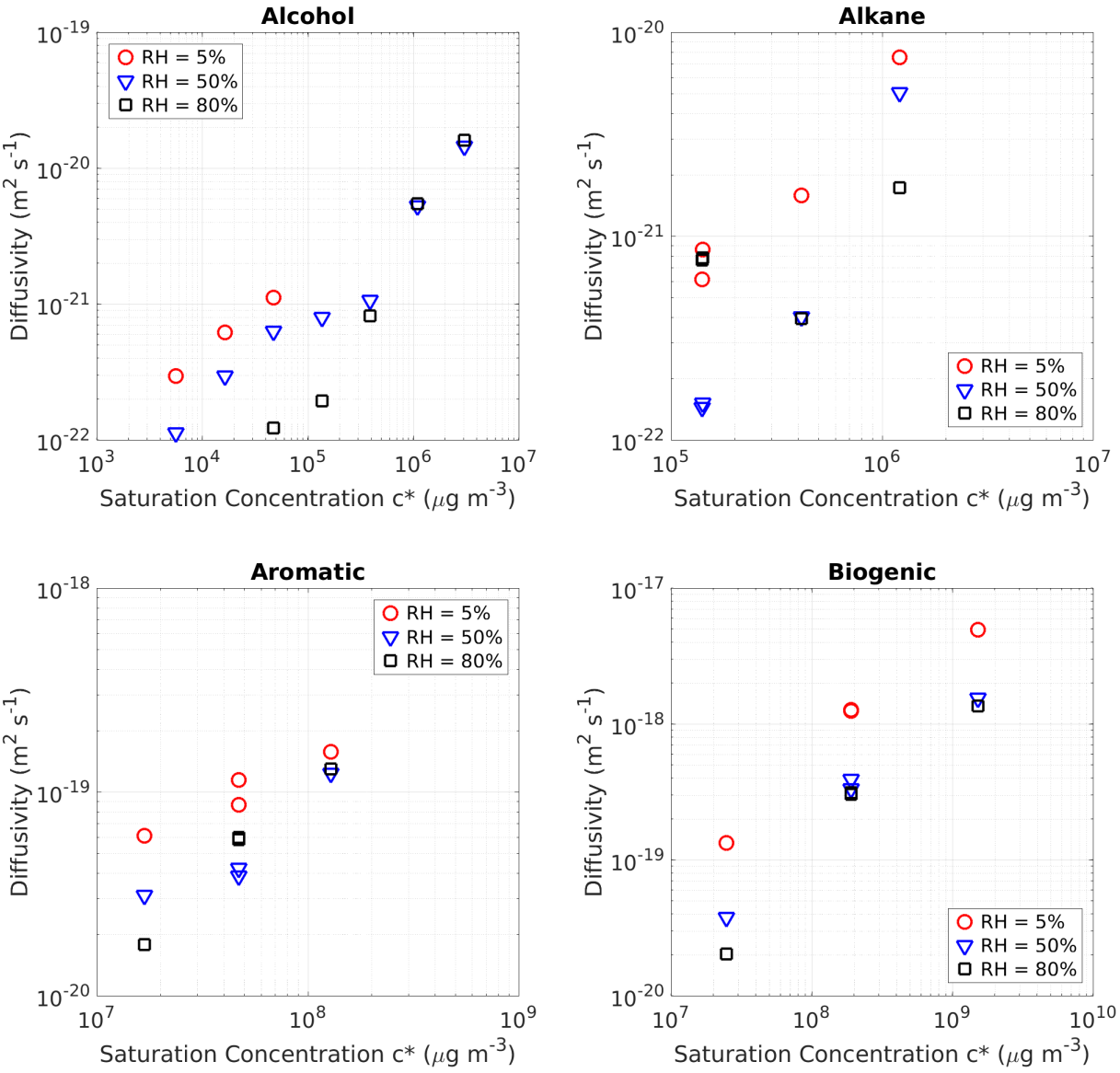

Figure S5: Inferred Diffusivity $\mathcal{D}_{\text{eff}}$ (m^2 s^{-1}) in FEP Teflon film as a function of saturation concentration c^* (μg m^{-3}) at different relative humidities for alcohols (C_6-C_{12} 1-alcohols), alkanes (C_{12}-C_{14} *n*-alkanes and *n*-octylcyclohexane), aromatics (toluene, *m*-, *o*-xylene, and 1,3,5-trimethylbenzene), and biogenic compounds (isoprene, MACR, MVK, and α-pinene).

VI. Exact and Approximate Solutions for the Kinetics of the System $\mathbf{X} \underset{\mathbf{k_{-1}}}{\overset{\mathbf{k_1}}{\rightleftharpoons}} \mathbf{Y} \xrightarrow{\mathbf{k_2}} \mathbf{Z}$

The system dynamics are described by the set of linear ODEs:

$$\frac{d}{dt}\mathbf{W} = \mathbb{A} \cdot \mathbf{W} \tag{S20}$$

where $\mathbf{W} = \begin{pmatrix} X \\ Y \end{pmatrix}$, and $\mathbb{A} = \begin{pmatrix} -k_1 & k_{-1} \\ k_1 & -k_{-1} - k_2 \end{pmatrix}$. It is assumed that X and Y rapidly come to equilibrium. The initial condition is $\mathbf{W}_0 = X_0 \begin{pmatrix} 1 \\ k_1/k_{-1} \end{pmatrix}$.

The eigenvalues of $\mathbb{A}$ are:

$$\begin{aligned} \lambda_1 &= \frac{-(k_1 + k_{-1} + k_2) - \sqrt{(k_1 + k_{-1} + k_2)^2 - 4k_1k_2}}{2} \\ \lambda_2 &= \frac{-(k_1 + k_{-1} + k_2) + \sqrt{(k_1 + k_{-1} + k_2)^2 - 4k_1k_2}}{2} \end{aligned} \tag{S21}$$

The solution of Eq. (S20) is

$$\frac{1}{X_0}\mathbf{W} = \frac{1}{X_0}\begin{pmatrix} X(t) \\ Y(t) \end{pmatrix} = -\frac{\lambda_2}{\lambda_1 - \lambda_2}\begin{pmatrix} 1 \\ \dfrac{k_1 + \lambda_1}{k_{-1}} \end{pmatrix} \mathrm{e}^{\lambda_1 t} + \frac{\lambda_1}{\lambda_1 - \lambda_2}\begin{pmatrix} 1 \\ \dfrac{k_1 + \lambda_2}{k_{-1}} \end{pmatrix} \mathrm{e}^{\lambda_2 t} \tag{S22}$$

And by mass balance:

$$Z(t) = X_0\left(1 - X(t) + \frac{k_1}{k_{-1}}(1 - Y(t)\right) \tag{S23}$$

Under conditions that $k_2 \ll k_1 + k_{-1}$, that is, rapid equilibrium established by X and Y, we can derive approximate solutions.

First, the eigenvalues can be simplified as:

$$\begin{aligned}\lambda_1 &= -(k_1 + k_{-1}) - \frac{k_{-1}}{k_1 + k_{-1}} k_2 \\ \lambda_2 &= -\frac{k_1}{k_1 + k_{-1}} k_2\end{aligned} \tag{S24}$$

We note that $\frac{\lambda_2}{\lambda_1} \ll 1$. If the equilibrium constant $K_{eq} = \frac{k_1}{k_{-1}} \gg 1$, $\lambda_1 = -k_1 - k_{-1}$ and $\lambda_2 = -k_2$. If $K_{eq} \ll 1$, $\lambda_1 = -k_1 - k_{-1} - k_2$ and $\lambda_2 = -\frac{k_1}{k_{-1}} k_2$.

Second, the slow change of X owing to the slow conversion of Y to Z is usually described in terms of a first-order rate constant k_w^X, in the units of time^{-1}:

$$\begin{aligned} k_w^X = \frac{1}{X}\frac{dX}{dt} &= \frac{\frac{\lambda_1\lambda_2}{\lambda_1 - \lambda_2} \mathrm{e}^{\lambda_1 t}\left(\mathrm{e}^{(\lambda_2 - \lambda_1)t} - 1\right)}{\frac{\lambda_1}{\lambda_1 - \lambda_2} \mathrm{e}^{\lambda_1 t}\left(\mathrm{e}^{(\lambda_2 - \lambda_1)t} - \frac{\lambda_2}{\lambda_1}\right)} = \lambda_2 \frac{\mathrm{e}^{(\frac{\lambda_2}{\lambda_1} - 1)\lambda_1 t} - 1}{\mathrm{e}^{(\frac{\lambda_2}{\lambda_1} - 1)\lambda_1 t} - \frac{\lambda_2}{\lambda_1}} \sim \lambda_2 \frac{\mathrm{e}^{-\lambda_1 t} - 1}{\mathrm{e}^{-\lambda_1 t}} \\ &= \lambda_2 \left(1 - \mathrm{e}^{\lambda_1 t}\right) \end{aligned} \tag{S25}$$

EQ. (S25) indicates that at the outset when t is small, the rate of change of X is $k_w^X \sim -\lambda_2\lambda_1 t$, which results in a relatively flat profile of X. As $t \to \infty$, $k_w^X \sim -\lambda_2$, suggesting that, X and Y can be viewed as a group, for which the net loss rate is λ_2.

VII. Application in Chamber Simulations

This two-layer model can be readily incorporated into models of vapor and particle dynamics in chambers, since only the fates of vapor molecules in gas phase and in the surface layer have to be tracked. The scheme $\mathrm{X} \underset{\mathrm{k_{-1}}}{\overset{\mathrm{k_1}}{\rightleftharpoons}} \mathrm{Y} \xrightarrow{\mathrm{k_2}} \mathrm{Z}$ can simplify this incorporation, where X is the gas-phase concentration of concern and Y corresponds to its concentration in the surface. Thus the ordinary differential equations for X and Y are:

$$\frac{dX}{dt} = -k_1 X + k_{-1} Y + \sum P_{iX} - \sum L_{iX} \tag{S26}$$

$$\frac{dY}{dt} = k_1 Y - k_{-1} Y - k_2 Y \tag{S27}$$

where $\sum P_{iX}$ and $\sum L_{iX}$ are the production and loss processes for gas-phase species X in the chamber, respectively, e.g. chemical reactions or interaction with particles.[17] Expressions for $\mathrm{k_1}$, $\mathrm{k_{-1}}$, and $\mathrm{k_2}$ can be found in Table 1.

Initial conditions are required to apply this model. We suggest that: if Compound X is introduced into the chamber through injection, the initial conditions for EQs. (S26) and (S27) are $X = X_0$ and $Y = X_0 \frac{k_1}{k_{-1}}$; if Compound X is generated in-situ chemically, the initial conditions are $X = Y = 0$.

Another key aspect is the value of $\mathrm{k_2}$. From Table 1, $\mathrm{k_2}$ can be found through $\mathcal{D}_{\mathrm{eff}}$, while $\mathcal{D}_{\mathrm{eff}}$ can be predicted based on the molecular volume (θ) and the vapor saturation concentration (c^*). If one wants to account for the history of use of the chamber, a rough expression for the corrected diffusivity is $\mathcal{D}_{\mathrm{eff}}^{corr} = \frac{0.015n}{330}\mathcal{D}_{\mathrm{eff}}$, where n is the number of experiments performed in that chamber, and we assume the diffusivity increases by $\sim 1.5\%$ per experiment based on the finding in Section IV. However, the semi-empirical expression for $\mathrm{k_2}$ applies only to dry conditions at room temperature and a chamber constructed of 50 μm Teflon film. For other conditions, e.g. different RH or temperature, we suggest that $\mathrm{k_2}$ be determined experimentally. One has to find the "apparent" first-order decay rate k_w^X by exponentially fitting the

experimental data, similar to the GC measurement in this study, and apply $k_w^X = \frac{k_1}{k_1 + k_{-1}} k_2$ to find k_2.

References

(1) Corner, J.; Pendlebury, E. D. The coagulation and deposition of a stirred aerosol. *Proc. Phys. Soc. B* **1951**, *64*, 645.

(2) Crump, J. G.; Seinfeld, J. H. Turbulent deposition and gravitational sedimentation of an aerosol in a vessel of arbitrary shape. *J. Aerosol Sci.* **1981**, *12*, 405–415.

(3) Seinfeld, J. H.; Pankow, J. F. Organic atmospheric particulate material. *Annu. Rev. Phys. Chem.* **2003**, *54*, 121–140.

(4) Zhang, X.; Cappa, C. D.; Jathar, S. H.; McVay, R. C.; Ensberg, J. J.; Kleeman, M. J.; Seinfeld, J. H. Influence of vapor wall loss in laboratory chambers on yields of secondary organic aerosol. *Proc. Natl. Acad. Sci. U. S. A.* **2014**, *111*, 5802–5807.

(5) Matsunaga, A.; Ziemann, P. J. Gas-wall partitioning of organic compounds in a Teflon film chamber and potential effects on reaction product and aerosol yield measurements. *Aerosol Sci. Technol.* **2010**, *44*, 881–892.

(6) Yeh, G. K.; Ziemann, P. J. Alkyl nitrate formation from the reactions of C8-C14 n-alkanes with OH radicals in the presence of NOx: measured yields with essential corrections for gas-wall partitioning. *J. Phys. Chem. A* **2014**, *118*, 8147–8157.

(7) Yeh, G. K.; Ziemann, P. J. Gas-wall partitioning of oxygenated organic compounds: measurements, structure-activity relationships, and correlation with gas chromatographic retention factor. *Aerosol Sci. Technol.* **2015**, *49*, 727–738.

(8) Krechmer, J. E.; Pagonis, D.; Ziemann, P. J.; Jimenez, J. L. Quantification of gas-wall partitioning in Teflon environmental chambers using rapid bursts of low-volatility oxidized species generated in situ. *Environ. Sci. Technol.* **2016**, *50*, 5757–5765.

(9) Compernolle, S.; Ceulemans, K.; Müller, J.-F. EVAPORATION: a new vapour pressure

193 estimation methodfor organic molecules including non-additivity and intramolecular
194 interactions. *Atmos. Chem. Phys.* **2011**, *11*, 9431–9450.

195 (10) Zhang, X.; Schwantes, R. H.; McVay, R. C.; Lignell, H.; Coggon, M. M.; Flagan, R. C.;
196 Seinfeld, J. H. Vapor wall deposition in Teflon chambers. *Atmos. Chem. Phys.* **2015**,
197 *15*, 4197–4214.

198 (11) Tropo, Vapour pressure of Pure Liquid Organic Compounds. `http://tropo.`
199 `aeronomie.be/models/evaporation_run.htm`.

200 (12) Pankow, J. F.; Asher, W. E. SIMPOL.1: a simple group contribution method for
201 predicting vapor pressures and enthalpies of vaporization of multifunctional organic
202 compounds. *Atmos. Chem. Phys.* **2008**, *8*, 2773–2796.

203 (13) McMurry, P. H.; Grosjean, D. Gas and aerosol wall losses in Teflon film smog chambers.
204 *Environ. Sci. Technol.* **1985**, *19*, 1176–1182.

205 (14) Bagley, E.; Long, F. A. Two-stage Sorption and Desorption of Organic Vapors in Cel-
206 lulose Acetate[1,2]. *J. Am. Chem. Soc.* **1955**, *77*, 2172–2178.

207 (15) Crank, J. A theoretical investigation of the influence of molecular relaxation and inter-
208 nal stress on diffusion in polymers. *J. Polym. Sci.* **1953**, *11*, 151–168.

209 (16) Loza, C. L.; Chan, A. W. H.; Galloway, M. M.; Keutsch, F. N.; Flagan, R. C.; Sein-
210 feld, J. H. Characterization of vapor wall loss in laboratory chambers. *Environ. Sci.*
211 *Technol.* **2010**, *44*, 5074–5078.

212 (17) Seinfeld, J. H.; Pandis, S. N. *Atmospheric Chemistry and Physics: From Air Pollution*
213 *to Climate Change*, 3rd ed.; Wiley Sons, 2016.